

Alma Mater Studiorum Università di Bologna
Archivio istituzionale della ricerca

A machine learning methodology for improving the accuracy of laminar flame simulations with reduced chemical kinetics mechanisms

This is the final peer-reviewed author's accepted manuscript (postprint) of the following publication:

Published Version:

Pulga L., Bianchi Gian Marco, Falfari S., Forte C. (2020). A machine learning methodology for improving the accuracy of laminar flame simulations with reduced chemical kinetics mechanisms. COMBUSTION AND FLAME, 216, 72-81 [10.1016/j.combustflame.2020.02.021].

Availability:

This version is available at: <https://hdl.handle.net/11585/756114> since: 2020-04-21

Published:

DOI: <http://doi.org/10.1016/j.combustflame.2020.02.021>

Terms of use:

Some rights reserved. The terms and conditions for the reuse of this version of the manuscript are specified in the publishing policy. For all terms of use and more information see the publisher's website.

This item was downloaded from IRIS Università di Bologna (<https://cris.unibo.it/>).
When citing, please refer to the published version.

(Article begins on next page)

A machine learning methodology for improving the accuracy of laminar flame simulations with reduced chemical kinetics mechanisms

L. Pulga^{a}, G.M. Bianchi^a, S. Falfari^a, C. Forte^b*

^a DIN Department of Industrial Engineering – University of Bologna, Via del Risorgimento 2, 40136 Bologna, Italy

^b NAIS s.r.l., Via M. Callas 4, 40131 Bologna, Italy

Abstract

The focus of the present work is to investigate a new methodology for the rapid generation of laminar flame speed lookup tables, to be used replacing correlation laws in internal combustion engine simulations. Current production engines run mostly under the thickened wrinkled flame combustion regime, which allows the application of a flamelet modelling approach, which requires the a-priori evaluation of the laminar flame speed and thickness. The use of correlation laws, derived from experimental data, has the advantage to be extremely fast to compute, but displays a lack of precision in conditions far from the experimental reference, as it usually happens for ICE applications. On the other hand, the detailed chemical simulation of a freely propagating adiabatic flame, performed for a sufficiently refined grid of reference points, to be interpolated during runtime, might require hundreds of hours of computing. The use of a reduced chemical mechanism can potentially cut by orders of magnitude the required time, but on the other hand it will decrease accuracy. In the present work, the potential of integrating machine learning algorithms and neural networks in the workflow with different approaches was valuated, leveraging the potential of new and optimized software libraries, to reduce simulation times while maintaining a high level of accuracy, with respect to the results obtained with the complete scheme.

Keywords

Laminar Flame Speed
Machine Learning
Reduced Mechanism

1. INTRODUCTION

Current production powertrains are systems characterized by a high level of complexity with the integration of hybrid components, turbochargers and pollutant reduction technologies. The trend of downsizing and down-speeding will significantly reduce fuel consumption and emissions, maintaining the same power output [1]. On the other hand, this approach is leading to an increase in the pressure and temperature reached inside the cylinder during the combustion phase. Numerical simulations play a key role in providing engine designers with a deeper insight into the performance of new configurations, but only if they can produce robust and reliable results in a reasonable amount of time. To maintain the fluid dynamics simulation within useful time constraints, RANS (Reynolds Averaged Navier-Stokes) is required, with motion and species transport models that account for the smaller scales. To simulate the firing cycle of an ICE several miscellaneous models are required, i.e. fuel injection, droplet break-up and droplet-wall interaction, liquid film, ignition, combustion and more, based on the level of detail that needs to be reached for the analysis.

Focusing on the ignition and combustion models that can be applied to the simulation of ICE's, and suitable for the RANS framework, the most adopted ones are based on the turbulent flamelet hypothesis [2], which states that the turbulent flames can be regarded as an aggregate of thin, one-dimensional laminar flamelets embedded within the turbulent flow field [2, 3]. This hypothesis still holds true if the interaction between turbulence and combustion time and length scales fall within a definite range, where the condition stating that fresh and burnt gases are always separated by a thin reacting interface, can be more realistically satisfied.

The interaction between flame and turbulence scales can be represented by the well-known Borghi's diagram, which also shows the limit of the applicability of flamelet combustion models. Considering the wide range of operating conditions, and the spatial distribution of fluid dynamics and chemical properties that the flame front faces in reciprocating internal combustion engines applications, it is worth underlining that the interaction between turbulence and chemistry length and time scales is always

* Corresponding Author. Email address: leonardo.pulga2@unibo.it

located between the wrinkled flamelets and the thickened wrinkled flame regions. This feature enables the application of the flamelet combustion models in RANS simulations of ICE's [2, 4, 5].

The laminar flames are described by two main characteristics, used as an input for the combustion model: laminar flame speed (s_L) and laminar flame thickness (l_F). These quantities vary as a function of the chemical parameters, i.e. mixture equivalence ratio, local exhaust gas mass fraction, and thermodynamics properties of the system, i.e. pressure (P) and temperature of the unburnt mixture (T_u).

2. CORRELATION LAWS APPROACH

The standard approach for the definition of the reference laminar flame speed and the laminar flame thickness, as input for a flamelet turbulent combustion model relies on the adoption of a correlation law. These functions are usually in the form reported in [6] and described by Equations 1-4:

$$s_L = s_L^0 \cdot \left(\frac{T}{T_0}\right)^\alpha \cdot \left(\frac{P}{P_0}\right)^\beta \cdot (1 - k \cdot X_{EGR}^\gamma) \quad (1)$$

$$s_L^0 = B_m - B_f (\phi - \phi_m)^2 \quad (2)$$

$$\alpha = \alpha_0 - \alpha_1(\phi - 1) \quad (3)$$

$$\beta = \beta_0 + \beta_1(\phi - 1) \quad (4)$$

In Equation 1, T_0 is the reference unburnt gas temperature and P_0 the reference pressure, usually taken at ambient conditions, the factor $k \cdot X_{EGR}^\gamma$ is a correction term introduced to account for the presence of EGR (Exhaust Gas Recirculation) as inert and k a constant of proportionality with values found in literature between 1.7 and 2.3 [4]. The coefficients in Equations 1-4 must be modified as a function of the chosen correlation (usually Metghalchi and Keck[6], Heywood [7] or Gülder [8]), and are written in literature for different surrogates and PRFs (Primary Reference Fuels), obtained through experimental campaigns, while ϕ_m indicates the equivalence ratio at which maximum laminar flame speed is reached at reference conditions.

Even though this kind of equation accounts for the main flow parameters affecting the flame laminar speed, the experimental validation has been performed only within a limited range of conditions, which are far from those occurring in current production turbo-charged SI-DI engines especially in terms of pressure and temperature. To bridge the gap of missing reference values at high temperature and pressure, more reference points are commonly generated using detailed chemical kinetics simulations of simplified systems (e.g. adiabatic axisymmetric stagnation flows). The outcomes of these simulations can be employed for the development of more accurate correlation laws, or to generate lookup tables that will be interpolated in runtime.

The second essential property of the laminar flames is the front thickness, which can be computed as the ratio between thermal diffusivity of the fresh gas and the laminar flame speed. A more useful definition of laminar flame thickness is given by [1] using the temperature profile, reported in Equation 5, where subscript 1 indicates the unburnt (fresh) mixture, and 2 indicates the burnt phase:

$$\delta_L^0 = \frac{T_2 - T_1}{\max\left(\left|\frac{dT}{dx}\right|\right)} \quad (5)$$

The definition and the evaluation of the laminar front thickness is notable since it affects the wrinkling efficiency of turbulence eddies. The chosen definition of laminar flame thickness in Equation 5 is described in [2] as thermal thickness, and it is reported as the most representative for laminar flames, but the application in the CFD simulations of ICEs is more complex, because of the several hypotheses made in the combustion and turbulence models.

3. GENERATION OF LOOK-UP TABLES OF LAMINAR FLAME SPEED AND THICKNESS FROM DETAILED CHEMISTRY SIMULATIONS

To compute a lookup table of laminar flame speed and thickness, a detailed simulation of a one-dimensional freely propagating planar adiabatic flame, with transport, thermodynamic and reaction properties for each species in the considered mixture are performed using the Cantera chemical solver implementation in Python [8], for a set of reference conditions.

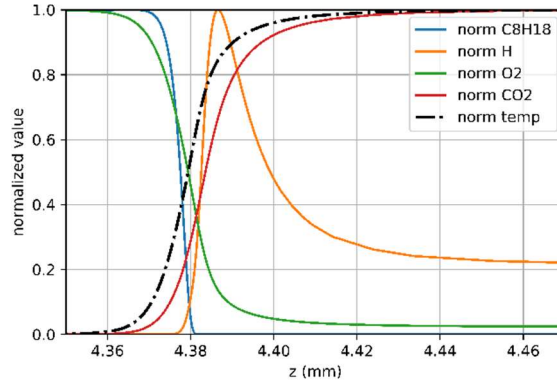


Fig. 1 Normalized profile of the mass fractions of C_8H_{18} , H , CO_2 and O_2 and normalized temperature of a freely propagating adiabatic flame at $P=40$ bar, $T=600$ K, $\phi=1$ and $EGR=0$ %.

Since the use of a lookup table should be applicable to both part load and WOT (Wide Opened Throttle) engine conditions, a wide range of pressure (from 1 bar to 145 bar) and unburnt temperature (from 400 K to 960 K) values must be considered. In addition, since the spatial distribution of the mixture can lead to very rich or very lean areas during the combustion process (equivalence ratio from 0.3 to 1.8), and to different distributions of the exhaust gases (EGR mass fraction from 0 to 0.3), it is also necessary to consider very different chemical compositions. From a first analysis, and referring to literature observations [4, 8], it was decided to use a refined grid along the axis that represent ϕ and T_{un} , whose values affect the laminar flame speed and thickness even for small changes, while keeping the number of reference points for pressure and EGR lower, for time requirements.

Tab. 1 Number of grid points necessary for a comprehensive lookup table along each direction, and variables' boundaries.

| | Min | Max | # Points |
|--------------|-----|-----|----------|
| P (bar) | 5 | 145 | 16 |
| T_{un} (K) | 400 | 960 | 28 |
| ϕ (—) | 0.3 | 1.8 | 16 |
| EGR (%) | 0 | 30 | 8 |

The total number of simulations to be performed is given by the full combinations of the reference data, i.e. 57344 points.

The chosen methodology for the definition of the lookup table is based on the work by Cazzoli et al. [4] and requires the iterative solution, with successive grid refinements, of a steady adiabatic free flame.

The laminar flame speed value is a property of the flame object in the programming framework of Cantera. Since the simulation is performed for a planar unstrained flame, the laminar flame speed is assumed to be equal to the consumption speed and to the displacement speed of the unburned gas next to the reaction zone [3]. The flame thickness is determined by using Equation 5 from the temperature profile across the flame front, inside the domain, as can be noticed in Figure 2.

Besides all the implementation details and the simulation methodology, which have been studied in previous works [4], the most relevant choice refers to the whole chemical kinetics mechanism adopted, once the fuel surrogate has been selected. The selection must keep into account three conditions:

- The presence of the species of the adopted fuel surrogate in the chemical mechanism;
- The presence of high and low temperature reactions parameters;
- The computational effort required for the problem solution (function of the number of species and reactions considered).

Since real engine CFD simulations are concerned, and due to the availability of experimental data [10], the selected fuel surrogate is the *TAE7000* (RON 98.1, composition: 13.7%v n-heptane C_7H_{16} , 42.9%v iso-octane C_8H_{18} , 43.4%v toluene C_7H_8), which was found to provide accurate laminar flame speed predictions to that of a TOTAL commercial gasoline [10].

The chosen surrogate fuel is composed of species that are considered in different available chemical kinetics schemes [4]. Four of them have been chosen for testing in the present study, as listed in Table 2, because of their extensively discussed validation in literature [4, 11, 12, 13, 14] and because they display different degrees of complexity in terms of number of species and reactions considered.

Tab. 2 Number of species and reactions present in each chemical kinetics mechanism tested, and estimated comparison of the time necessary for running each simulation.

| | Time/Sim | # Species | # Reactions |
|-------------|-----------|-----------|-------------|
| POLIMI red. | REF | 156 | 3465 |
| POLIMI | ~6 x REF | 451 | 8153 |
| LLNL323 | ~6 x REF | 323 | 2606 |
| LLNL | >20 x REF | 1387 | 10481 |

The LLNL mechanism [14] and the POLIMI [11] are assumed to be representative of complete mechanisms, considering the number of species and reactions involved, as it is shown in Table 2, as far as the laminar flame speed calculations are concerned. The POLIMI reduced [13], and the LLNL323 [14] are considered reduced mechanisms, which however, are expected to represent both the low and the high temperature conditions. These differences cause a great unbalancing in terms of the CPU time required for simulating a single reference condition. The comparison of computing times has been performed averaging ten simulation points with different conditions on the same machine having the following hardware and software configuration: Intel Xeon Platinum 3.0 GHz, 36 cores and 144 GB ram, Cantera version 2.3.0 on Python 3.7.2.

Due to its time cost requirements, the POLIMI complete chemical kinetics scheme has been chosen as reference, following the conclusion of [5]. The comparison of the results of the detailed mechanism with the reduced form for a condition with experimental data available [4] shows that the latter displays a lack of accuracy in the region of equivalence ratio that is of highest importance for internal combustion engine application ($0.7 < \phi < 1.3$).

The choice of the mechanism must be based on the trade-off between time required and accuracy of the results with respect to validated reference values. The aim of the following sections and the contribution of the paper are to outline a methodology for the integration of reduced and complete chemical kinetics schemes, for coupling both low time cost requirement and the accuracy of the detailed chemical simulations, thanks to the integration of a machine learning algorithm into the workflow.

4. POSSIBLE MACHINE LEARNING INTEGRATION APPROACHES

The application of machine learning algorithms to chemistry tabulation for the application in CFD codes has been investigated in literature, particularly regarding the generation of more accurate correlations [15] or to provide more precise algorithms to fit the results obtained from ISAT (In Situ Adaptive Tabulation [16]) in runtime [17].

The possible approaches to integrate a machine learning model with detailed chemistry simulations to generate new tabulation points, proposed and analysed in the present work, can be classified with respect to the level of autonomy that is given to the model.

Two opposite simulation approaches would be:

- Train a machine learning model on the available results (a few points of the simulation grid) and use it to construct autonomously the full simulation grid. From now, this will be referred to as '*Machine Learning Regression*';
- Perform detailed chemical simulations for the full simulation matrix and employ a machine learning algorithm to compensate the missing values.

The former approach, the '*Machine Learning Regression*', works similarly to a correlation law, thus sharing its positive and negative aspects. It is quite fast to compute, since the required time is the sum of the simulation time (for reference points) and the training of the ML model, but it relies only on the performance of the model, even for points far from the training set. This approach will be tested and evaluated in the next sections using different machine learning algorithms and neural network architectures.

On the other hand, the latter approach, i.e. the full matrix simulation, is extremely time consuming if one needs to perform a relevant number of simulations ($\sim 10^4$) since the role of machine learning is found to be marginal in the process, leading to no effective improvement.

In the present research, an alternative simulation approach is proposed and from now it will be referred to as ‘*Accuracy Recovery*’. It is based on the observation that it is possible to perform chemical simulations with different degree of detail, with respect to the number of reactions and species considered. The use of a reduced scheme can lead to a drastic decrement of the simulation time, as reported in Table 2, but it also leads to a less precise prediction of the output values, as shown in the next sections.

The idea of the proposed approach is to overcome the shortcoming of using a reduced scheme by adding a correction term (η) to the simulation output. This term can be estimated by a machine learning algorithm trained on available data.

$$\tilde{s}_L = (s_L)_{1D_red} \cdot (1 + \eta_{ML}) \quad (6)$$

In Equation 6 \tilde{s}_L represents the corrected laminar flame speed, obtained by integrating the value $(s_L)_{1D_red}$, i.e. the laminar flame speed obtained with the reduced chemical kinetics scheme, and η_{ML} , which is the relative error estimated by the machine learning algorithm as a function of the physical and chemical properties of the simulated point.

The use of the correction term is expected to compensate most part of the error committed by the reduced scheme, but in a fraction of the time that a simulation with the complete scheme would require, leading to an optimal trade-off between computation time and accuracy.

In order to compute an estimate of the accuracy correction term (η_{ML}) for a given combination of input parameters, the ML model must be trained on the available dataset of both reduced and full chemical simulations at the reference points. A deeper analysis of the modelling aspects for the error estimation will be reported in the next sections.

Independently from the chosen strategy, the features that the chosen model must have are the following:

- Since the output is a value and not a category, it must be a regression model [18];
- Training data must be available with both features and outputs, making it a supervised machine learning problem;
- The model should be able to capture non linearities;
- Since the aim of the approach is to keep the number of the simulations with the complete scheme as low as possible, the model should be characterized by low bias, in order to avoid excessive overfitting [18];
- For the same reason, the model performance should reach acceptable levels of accuracy with a limited number of training samples.

In addition to these features, the proposed workflow must be capable of removing outliers, since some differences between the reduced and the detailed chemical simulation results could be caused by numerical errors and not related to the use of one scheme or the other.

5. THEORY OF THE EMPLOYED MACHINE LEARNING ALGORITHMS

The current section will introduce the two algorithms that reached the best performances in the presented application, with a focus on their features and tuning parameters. The implementation of these models relies on open-source software libraries available for Python 3.7.2, Tensorflow [19] for the ANNs adopted and Scikit-learn [20] for pre-processing the data and for the other machine learning models.

Ensemble regressors (Adaboost):

The idea of boosting has been introduced by Freund [21] and Zhu [22] and it is considered one of the most common and efficient strategies for machine learning projects. An implementation available in literature, and already implemented in the adopted library, is ADaptive BOOST (also known as Adaboost). The purpose of an ensemble method is to turn a set of weak learners, i.e. models that perform slightly better than random guess, into a better model, by combining their outputs. The underlying idea of the algorithm is to subsequently train a series of weak learners, changing the weight of each training samples in the dataset, based on the performance of the previous learners on that point. In this way, a higher attention will be given to those features of the training set that the previous learning models did not capture, and finally perform a weighted sum of all the weak models.

The parameters that mostly influence this algorithm are:

- The type of base regressor employed (often a regression tree due to its simplicity [23]);
- The number of weak learners adopted;
- The learning rate, i.e. a term to scale the contribution of each learner in the final output.

After some internal testing, it has been decided to maintain the learning rate constant (set to 1.1, to slightly accelerate the training phase) and the type of base regressor (regression trees with variable depth), since variations in these two parameters did not affect significantly the result, while the number of base regressors is maintained variable in the range 10 – 500.

The Regression Tree is a supervised regression model, based on a tree-like graph, in which each internal node represents a condition on an attribute, each branch represents the output of the ‘test’, and the leaves correspond to the output obtained by terminal nodes in the training data, which is the mean response of observations falling in that region of the attributes domain.

Neural Network (Deep learning):

An artificial neural network is a network of simple elements called neurons, which receive an input, change their internal state (activation) according to that input with an imposed function, and produce an output to the connected neurons, or to the final node, depending on the input and activation function used. The layers of neurons can be distinguished based on the distance from the input neurons in terms of connections, and they are divided into input layer, output layer, which is the final step, and hidden layer(s) that are located between the previous two. Since there are 4 variables (pressure, temperature of the fresh mixture, equivalence ratio and EGR mass fraction), the number of neurons in the input layer is fixed, and the output layer must be constituted of 1 neuron, since the output of the algorithm is represented by a single value. In terms of topology, the parameters that can affect the performance of a model are depth of the network (i.e. the number of hidden layers) and width of the hidden layers (i.e. number of neurons per layer). The other parameters that can be tuned to obtain better results are:

- The activation function for each layer;
- The optimization algorithm used during training;
- The number of epochs available during training (or the possibility of early stopping);
- The batch size of the data fed to the network during each phase of training.

During the presented activity it was defined and maintained a reference value for the optimization algorithm (*Adam* [18]), for the number of epochs (10000, which is a high value, but the integration with early stopping, in case the loss would not descend for more than 5 successive iterations, was enough to maintain the time required for training acceptable) and the batch size (about 20% the size of the chosen training dataset). The variables explored are related to the topology of the network, and to the activation functions (*tanh* or *relu* [18]).

6. APPLICATION OF THE MACHINE LEARNING REGRESSION

The first methodology relies entirely on the output of the model to obtain a value for laminar flame speed and thickness, which is then applied as a ‘complex interpolation algorithm’. In order to capture all nonlinearities, and thanks to the availability of a large dataset, after preliminary tests with all selected algorithms, it has been chosen to focus only on the optimization of a neural network for this application, and on the evaluation of the impact of the number of points employed during the training phase. The features of the tested neural networks are reported in Table 3.

Tab. 3 Main features of the 5 neural network topologies used.

| | NN1 | NN2 | NN3 | NN4 | NN5 |
|-----------------|-------------------------------|-------------------------------|-------------|-------------|-------------------------------|
| Layers | 7 | 4 | 4 | 4 | 8 |
| Nodes | 57 | 17 | 17 | 17 | 29 |
| Activ. Func. | <i>Tanh</i> <i>Relu(5)</i> | <i>Tanh</i> <i>Relu(2)</i> | <i>Tanh</i> | <i>Relu</i> | <i>Tanh</i> <i>Relu(6)</i> |

Considering that the first layer represents the input step and the last layer is constituted by the only output neuron, the minimum number of hidden layers used is 2, in NN2, NN3 and NN4, that differ in the activation function used for each but the last layer (a combination of *tanh* and *relu* functions). NN5 presents a deeper architecture, which however does not increase in width, while NN1 is a more complex network, with larger layers, whose structure is represented graphically in Figure 2.

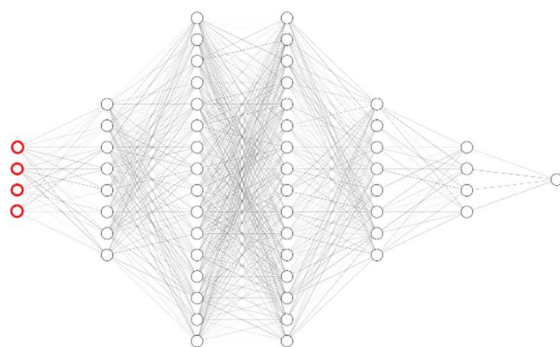


Fig. 2 ANN architecture 1, activation function = *relu* for white circles and *tanh* for red circles, optimizer=Adam, 5 hidden layers and a total of 57 neurons.

Since the aim of the study was the optimization of the time requirements to perform all the simulations needed, the performance of each network was compared with a different number of training data, splitting the available dataset in a training set and a test set, with different proportions. The results reported in Figure 3 represent the mean absolute relative error performed by each configuration of ANN on the test set, as a function of the dataset splitting. The training step has been computed on the complementary dataset, and the split has been performed in order to present similar distributions of laminar flame speed for both sets.

The choice of the points for the training dataset in the “localized” split is, instead, based on a reasoned choice of representative thermodynamic conditions on an almost evenly distributed grid, that has also been adopted for the second methodology.

The values of the dataset were first normalized with 0 as mean value and a standard deviation of 1, and successively split, in order to have in the training set 50%, 20%, 5% and about 2% of the points available in the dataset.

7. RESULTS OBTAINED WITH MACHINE LEARNING REGRESSION

The number of epochs for the training of the coefficients of each ANN has been set to 10000 with early stopping, as explained in section 5, and the batch size was adapted to the size of the training set. The mean absolute relative error highlights the importance of the number of points regardless of the architecture, even if it gains more relevance with a deeper network (NN5), or when only *relu* is used as activation function (NN4). When the training set is too small, considering the distribution of the values of laminar flame speed, the training phase is not capable of even fitting all the training values, and performs poorly when applied to the test set. The difference between the successive errors is not extremely sensitive to the size of the training set for NN1 and NN2, because the chosen points are found to be well representative of the full data-grid.

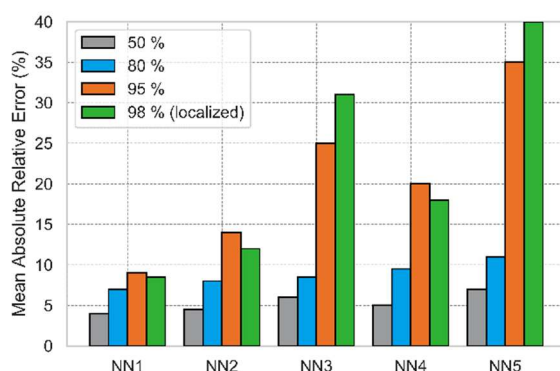


Fig. 3 Test error committed by different neural network topologies, with respect to different split methodologies of the laminar flame speed dataset.

Considering that the mean absolute relative error obtained by using the reduced scheme calculated on the whole dataset is 10.3%, the only neural network architecture capable of falling under that limit is NN1. The profile as a function of the equivalence ratio on three reference conditions is reported in Figures 4 and compared with that obtained with the complete and reduced chemical

kinetics schemes. The trained neural network appears to outperform the results obtained with the reduced scheme, with respect to the reference values, but the time required to calculate the full training dataset, compared to the estimates of Table 2, represents a significant drawback of this methodology.

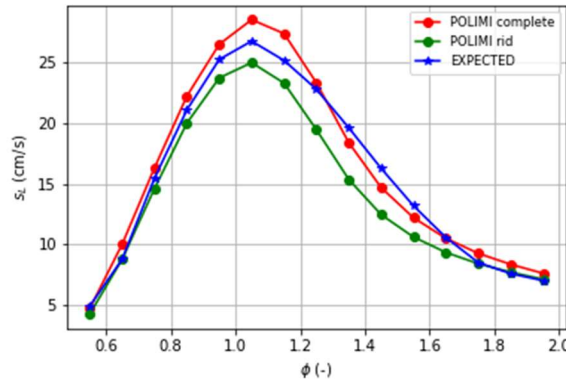


Fig. 4 S_L obtained with the complete chemical kinetics scheme (red), the reduced scheme (green) and the estimation with the best performing NN (blue), for EGR=0%, $P=105$ bar, $T=840$ K.

By analysing more in detail the performance of NN1 with respect to the train test size it emerges that, even if the mean absolute relative error is below the error committed by the reduced chemical mechanism, the dispersion of the error (identified with the standard deviation) is more than two times higher than that of the reduced mechanism, independently from the train set size, as reported in Figure 5.

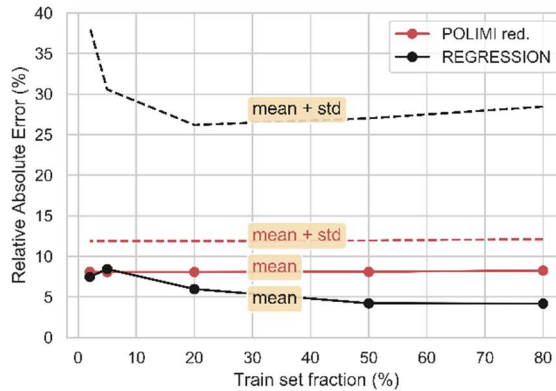


Fig. 5 Performance of NN1 as a function of train set size, compared with the reduced chemical kinetics scheme.

8. APPLICATION OF THE ACCURACY RECOVERY

The second methodology consists in the use of a model, whose input variables are the physical and chemical properties of the simulated points, to estimate the correction that must be applied on the results obtained with the reduced chemical kinetics scheme, in order to reduce the error with respect to the reference solution provided by the complete scheme.

Before addressing the proposed solution, the differences in the results obtained with the complete and the reduced schemes in terms of laminar flame speed and thickness must be analysed.

A simulation performed on the same hardware with the full POLIMI scheme is six times longer than that achieved by using the reduced mechanism, as reported in Table 2. The relative difference between the results of the simulations performed with the reduced and the complete chemical kinetics scheme behaves non-linearly with the physical and chemical properties of the simulated points. From a preliminary analysis on a dataset of about 6000 points, the relative error committed by using the reduced mechanism (with respect to the solution provided by the reference complete mechanism using *TAE7000* as representative fuel) behaves almost exponentially with pressure and temperature variations, as reported in Figure 6 only within a given range of equivalence ratio and EGR percentage. On the opposite, such an error is parabolic with respect to mixture composition, as

reported in Figure 7. On the other hand, outside of this confidence range, the behaviour tends to become not linear also with respect to pressure and temperature.

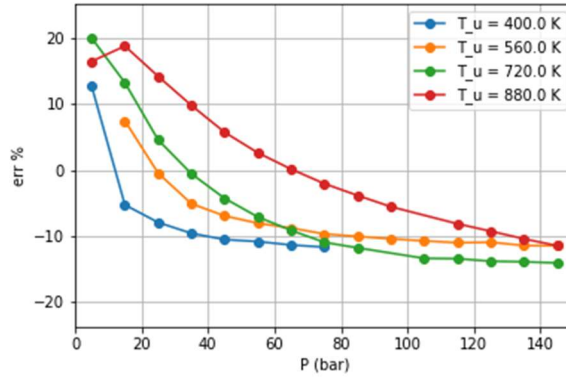


Fig. 6 Relative difference between laminar flame speed obtained with complete and reduced chemical kinetics scheme for different values of P and T , at $\phi=0.6$, $EGR=0\%$.

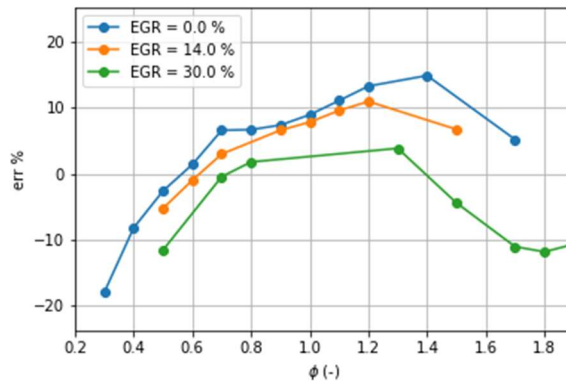


Fig. 7 Relative difference between laminar flame speed obtained with complete and reduced chemical kinetics scheme for different values of EGR and ϕ , at $P=105$ bar, $T=840$ K.

The workflow adopted for evaluating the best performing machine learning algorithm and tuning parameters, among regression tree, Adaboost, gradient boosting and support vector regression (which are other two common algorithms [16]) or neural network architecture (using the same five networks presented in Table 3) to be applied on the second methodology was constituted by the following steps:

- Calculate new output variables (relative error) from laminar flame speed and thickness values;
- Calculate mean and standard deviation and remove points outside limits, since the error can be due to numerical reasons in very lean or high pressure zones (chosen points where normalized error is outside a threshold of 3 standard deviations);
- Normalize the features of the remaining points with mean = 0 and standard deviation = 1;
- Split the dataset into train set, composed by about 2% of the available points 'localized' as described in the previous Section and reported in Figure 8 for a given combination of temperature and EGR mass fraction, and test set, composed by the remaining 98% of simulated points;
- Train the machine learning models and the neural networks with different topologies on the training set with different tuning parameters;
- Evaluate the model performance on the train set, on the test set and on a new evaluation set, made up of 45 points obtained at different conditions from those available in the dataset (ϕ from 0.45 to 1.95, $EGR=18\%$, and 3 combinations of pressure and temperature that can be reached during engine combustion simulations).

The model overall performance (referred to as J in Equation 8) represents a weighted sum of the relative mean error and maximum error, because, in a laminar flame lookup table, strong discontinuities like those introduced by a large maximum error in the correction step, could cause instabilities in the combustion simulations.

$$J = \sum_{i=\{train,test,eval\}} \alpha_i \cdot (0.8 \cdot E_{L1} + 0.2 \cdot E_{L\infty}) \quad (8)$$

The values of α_i are the weights attributed to each dataset in the overall evaluation. It is necessary to compute a weighted mean of the performance measures on the available datasets because, even though the test set contains the 98% of the data available, the poor predictions in some well-defined and limited regions of the full grid can lead to choosing a model which performs slightly better in those points, but more poorly in the remaining grid. On the other hand, the training set was selected specifically in order to represent, with its features, the properties of the full grid. Finally, the validation set was considered necessary to ensure that the selected model was not overfitting the training and the test sets. The assigned values of α are 0.3 for the training set, 0.6 for the test set and 0.1 for the validation set.

To highlight the distribution of the training points, with respect to the distribution of the absolute relative error in the ϕ -P plane at $T=960$ K and $EGR=0\%$, its value is reported in Figure 8. It can be noticed that the points of the training set represent intermediate and extreme values with a refinement where the gradient of the error is expected to be higher for temperature and equivalence ratio. On the other hand, it was chosen not to focus the training set on the regions with the highest errors (namely, high pressure and lean mixture, or low pressure and rich mixture), because their value, extremely localized in those regions, cannot be fully ascribed to the difference between the two chemical kinetics schemes and the value of the error in those points could have misled the model training.

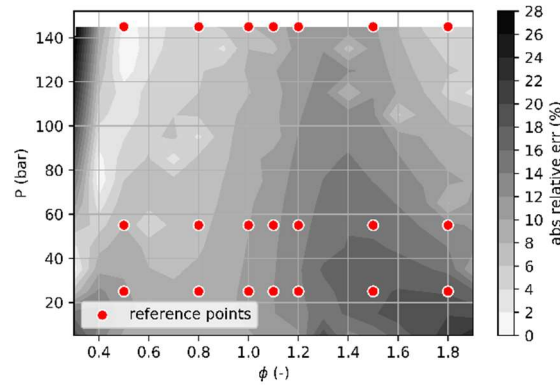


Fig. 8 Relative difference between laminar flame speed obtained with the complete and reduced chemical kinetics schemes on the ϕ -P plane, at $T=960$ K, $EGR=0\%$. The red dots are the simulated points used for the training of the machine learning algorithm.

9. RESULTS OBTAINED WITH THE ACCURACY RECOVERY

The results obtained by comparing the performance of the analysed algorithms for the second methodology have led to different conclusions concerning laminar flame speed and thickness prediction. For the former, NN1 (the same architecture used for the first methodology, reported in Table 3 and represented in Figure 3) has shown the best performance, while for the latter, the best model resulted to be Adaboost with the parameters collected in Table 4.

Tab. 4 Main features of Adaboost regressor obtaining the best performance for laminar flame thickness correction.

| Base Estimator | Decision Tree (Regressor) |
|----------------|---------------------------|
| Max Depth | 100 |
| # Estimators | 200 |
| Learning rate | 1.1 |
| Loss | Exponential |

The values of laminar flame speed for the validation set are reported in Figure 9 in comparison with the reference values obtained with the complete and reduced schemes. The results show a good performance, not only limited to the intermediate values of equivalence ratio, but to the full range of parameters analysed.

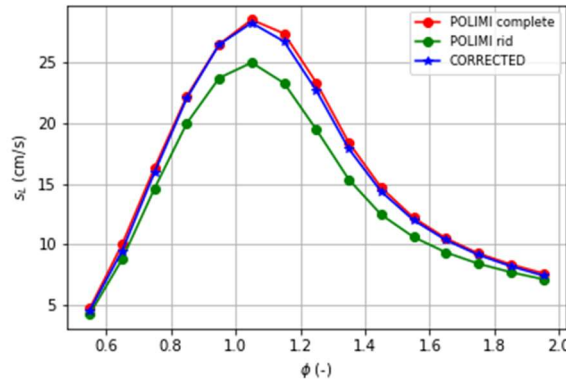


Fig. 9 Comparison of the laminar flame speed obtained with the complete chemical kinetics scheme (red), the reduced scheme (green) and the combination of reduced scheme and correction predicted by ML model (blue), for $P=20$ bar, $T=595$ K, $EGR=18\%$.

From the analysis of the error distribution of the laminar flame speed and thickness in the test set (Figures 10 and 11), obtained by employing the reduced chemical kinetics scheme and the correction algorithm, two benefits of the presented methodology emerge:

- the median relative error committed by the integrated approach decreases from -7.39% to 0.53% (laminar flame speed), and from 9% to 0% (laminar flame thickness);
- the error distribution shows a smaller variance in both applications, where 95% of the points in the test set fall under an absolute value of 5% error after correction.

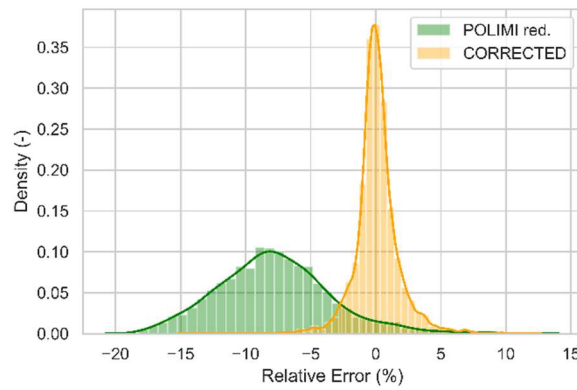


Fig. 10 Comparison of the relative error distribution between reduced and detailed chemical kinetic scheme, before (green) and after (orange) the application of the proposed methodology for laminar flame speed.

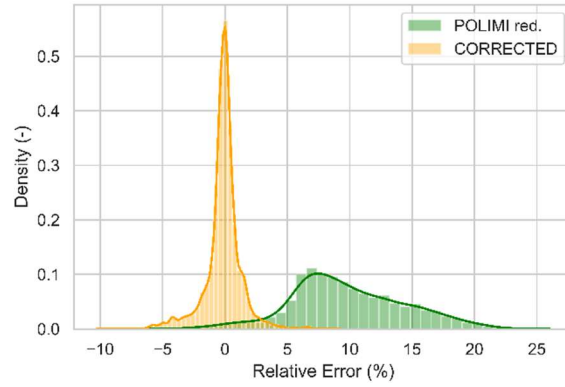


Fig. 11 Comparison of the relative error distribution between reduced and detailed chemical kinetic scheme, before (green) and after (orange) the application of the proposed methodology for laminar flame thickness.

The RMSE (Root Mean Squared Error) and the maximum relative error reported in Table 5 underline, however, the fact that the presented methodology is not capable of overcoming the strongest drawbacks of the reduced models in definite regions.

Tab. 5 Relative error indicators for laminar flame speed and thickness calculated between the complete scheme and the reduced scheme, with and without machine learning correction.

| | <i>Red. scheme</i> | <i>Red. + ML correction</i> |
|-------------------|--------------------|-----------------------------|
| s_l | | |
| <i>Median err</i> | -7.39 % | 0.53 % |
| <i>RMSE</i> | 13.05 % | 7.66 % |
| <i>Max err</i> | 36.10 % | 37.35 % |
| l_f | | |
| <i>Median err</i> | 9.00 % | 0.00 % |
| <i>RMSE</i> | 14.55 % | 5.02 % |
| <i>Max err</i> | 32.06 % | 25.34 % |

Even though this is most likely due to the fact that the training phase has been performed on a grid with a very limited number of points, to reduce the time requirements, it is also clear that some simulation points can be erroneously predicted because of numeric errors, while performing laminar flame simulations, especially for very lean or rich mixtures at high pressures, where the maximum errors are located both before and after the correction step. These regions, however, are unlikely reached during ICE computations, and are therefore considered acceptable.

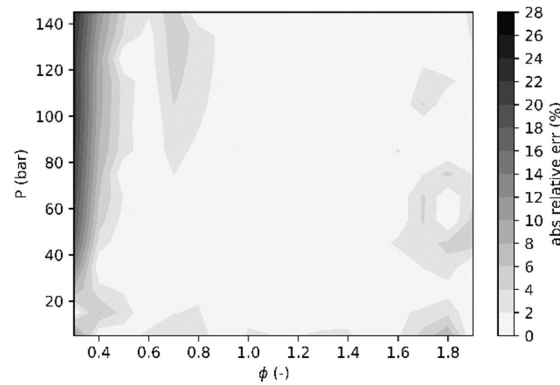


Fig. 12 Relative error distribution after the correction step for laminar flame speed on the ϕ - P plane, at $T=840$ K, $EGR=0$ %.

The dependence of the performance of the accuracy recovery methodology on the train set size is displayed in Figure 12, compared to the original error committed by the reduced mechanism. Independently from the train set size, the application of the correction algorithm is capable of reducing the mean absolute relative error to below 2% with respect to the laminar flame

speed values calculated with the complete mechanism. The distribution of the error, identified with the standard deviation, is also reduced thanks to the application of the correction algorithm with respect to the initial dataset.

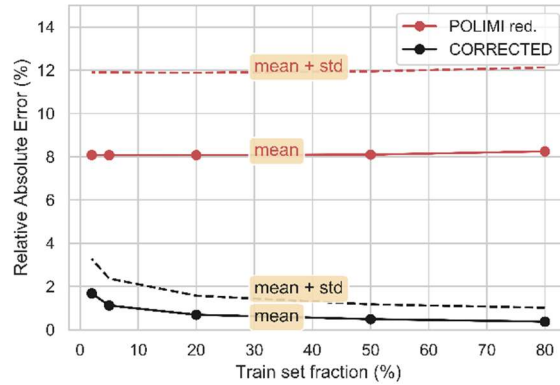


Fig. 13 Performance of the accuracy recovery method as a function of train set size, compared with the reduced chemical kinetics scheme.

10. COMPARISON WITH EXPERIMENTAL DATA

Since the results described in the present work apply to engine relevant conditions, the training and validation phases were performed on a grid with minimum temperature and pressure that are rarely reached during experimental tests with surrogate fuels [10]. Nevertheless, experimental data for the laminar flame speed of surrogate fuels at lower initial temperature and pressure conditions are available in literature, and the accuracy of the presented methodology can be further investigated with respect to those results. Following the work of Cazzoli et al. [4], and of Dirrenberger et al. [10], it has been made a comparison between the values of laminar flame speed for the surrogate fuel reported in Section 3 (TAE7000 [10]) obtained experimentally in a flat flame adiabatic burner at atmospheric pressure and initial temperature of 358 K with the results of 1D chemical simulations performed with the complete POLIMI mechanism and the reduced form. The results of the reduced scheme were finally integrated with the output of the neural network that was previously trained, without any additional adjustments. The results confirm the previous observations; that the proposed methodology can increment the accuracy in the computation of laminar flame speed, reducing the difference between the output of a reduced mechanism and a complete one at a time cost typical of the former one, once the machine learning algorithm is trained.

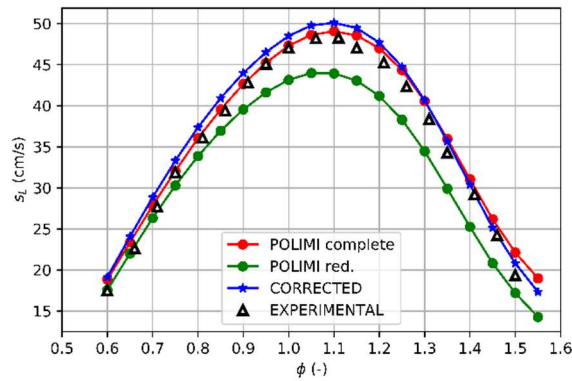


Fig. 14 Laminar flame speed calculated with POLIMI chemical kinetics full scheme and reduced scheme with and without correction, compared to experimental data [10] for a surrogate fuel at different equivalence ratios at ambient pressure, no dilution and initial temperature of 358 K.

11. CONCLUSION

In the present research the integration of machine learning and deep learning algorithms into a combustion simulation workflow has been analysed, in order to increase speed of computation, while keeping the accuracy within an appropriate range. The use of laminar flame speed table, obtained with 1D detailed chemistry simulations, is recognized as an improvement in the accuracy of flamelet combustion models [4, 5], but its computation time requirements prevent it from being a standard practice. Different

strategies of integration, and the most relevant parameters of each methodology, have been tested, and the results of the most promising approaches have been shown. It has been demonstrated that the proposed methodology can decrease the error committed by using a reduced chemical kinetics scheme in place of the complete version by employing a pre-trained machine learning algorithm, with proper features. The same methodology, applied to the laminar flame thickness, as computed by [2], leads to an even better result, with a median error committed near 0%. The only shortcoming of the proposed approach is the fact that, in very lean conditions ($\phi < 0.5$) the applied correction is almost ineffective, due to the fact that the training set does not contain points in that region, due to the requirement for it to be as general as possible.

Thanks to the proposed methodology, the time required to generate a laminar flame speed (and laminar flame thickness) lookup table with accuracy close to that reached by a complete chemical kinetics mechanism (mean absolute relative error below 1%) can be reduced by more than 80% with respect to the time required by using the POLIMI complete scheme. The overhead computing time required for running the simulations necessary to train the ML model becomes less relevant with increasing size of the full dataset up to less than 1% in the case of the grid considered in section 3, consisting of more than 50000 points, leading to an overall time reduction of 82.1% for the whole generation workflow.

12. FUTURE WORK

Since the authors have access to a previously computed laminar flame lookup table on an extensive data grid, computed with POLIMI full and reduced mechanisms, the results displayed in the present work refer to only one surrogate fuel and only one reduced chemical kinetics mechanism. Considering that the proposed methodology is intended to be robust to chemical properties variations, it is planned to investigate the performance of the model on more surrogates and reference fuels, training the coefficients on the new collected data, or without the additional training phase (analysing the opportunity to adopt the previously trained algorithm on new datasets). In addition, it is expected that the relative difference distribution is dependent on the methodology adopted for the reduction of the chemical kinetics scheme. This leads to the requirement for further validation of the robustness of the algorithm with respect to the approach used to generate the reduced mechanism.

An integrated methodology is also under development, with the aim of reducing chemical kinetics schemes, based on the DRGEP approach (Directed Relational Graph with Error Propagation [24]), where the performance measure, with respect to the full scheme, is not based on the error committed by the reduced scheme alone, as performed in standard practice [24] but by the full workflow presented in this work, which is expected to further allow the reduction of the number of species and reactions needed to obtain sufficiently accurate results in terms of laminar flame speed and thickness.

ACKNOWLEDGMENTS

The authors gratefully acknowledge support by NAIS s.r.l. for the research activity.

BIBLIOGRAPHY

- [1] Stanton, D., "Systematic Development of Highly Efficient and Clean Engines to Meet Future Commercial Vehicle Greenhouse Gas Regulations", SAE Int. J. Engines 6(3):1395-1480, 2013, DOI: 10.4271/2013-01-2421.
- [2] Poinot, T., Veynante, D., Theoretical and Numerical Combustion, 2001, Edwards, 9781930217058
- [3] Bray, K.N.C., Cant, R.S., Phillips, J.O.W., Williams, D., "Some applications of Kolmogorov's turbulence research in the field of combustion", 434th Proceedings of the Royal Society of London, Series A: Mathematical and Physical Sciences, DOI: 10.1098/rspa.1991.0090
- [4] Cazzoli, G., Forte, C., Bianchi, G., Falfari, S. et al., "A Chemical-Kinetic Approach to the Definition of the Laminar Flame Speed for the Simulation of the Combustion of Spark-Ignition Engines", SAE Technical Paper 2017-24-0035, 2017, DOI: 10.4271/2017-24-0035.

- [5] Del Pecchia, M., Breda, S., D'Adamo, A., Fontanesi, S. et al., "Development of Chemistry-Based Laminar Flame Speed Correlation for Part-Load SI Conditions and Validation in a GDI Research Engine", *SAE Int. J. Engines* 11(6):715-741, 2018, DOI: 10.4271/2018-01-0174.
- [6] Metghalchi, M., Keck, J., 1982. "Burning velocities of mixtures of air with methanol, isooctane, and indolene at high pressure and temperature". *Combustion and Flame*, 48(C), pp. 191-210.
- [7] Heywood, J. B., 1988. "Internal Combustion Engine Fundamentals", McGraw-Hill, New York
- [8] Gülder, Ö., 1982. "Laminar burning velocities of methanol, ethanol and isooctane-air mixtures". *Symposium (International) on Combustion*, 19(1), pp. 275-281.
- [9] Cantera: An object-oriented software toolkit for chemical kinetics, thermodynamics, and transport processes. <http://www.cantera.org>
- [10] Dirrenberger, P., Glaude, P.A., Bounaceur, R., Le Gall, H., Pires da Cruz, A., et al., "Laminar burning velocity of gasolines with addition of ethanol", *Fuel*, Elsevier, 2014, 115, pp.162-169. DOI: 10.1016/j.fuel.2013.07.015
- [11] Ranzi, E., Frassoldati, A., Grana, R., Cuoci, A., Faravelli, T., Kelley, A.P., Law, C.K., "Hierarchical and comparative kinetic modelling of laminar flame speeds of hydrocarbon and oxygenated fuels", *Progress in Energy and Combustion Science*, 38 (4), pp. 468-501 (2012), DOI: 10.1016/j.pecs.2012.03.004
- [12] Stagni, A., Cuoci, A., Frassoldati, A., Faravelli, T., Ranzi, E., "Lumping and reduction of detailed kinetic schemes: An effective coupling", *Industrial and Engineering Chemistry Research*, 53 (22), pp. 9004-9016 (2014), DOI: 10.1021/ie403272f
- [13] Ranzi, E., Frassoldati, A., Stagni, A., Pelucchi, M., Cuoci, A., Faravelli, T., "Reduced kinetic schemes of complex reaction systems: Fossil and biomass-derived transportation fuels", *International Journal of Chemical Kinetics*, 46 (9), pp. 512-542 (2014), DOI: 10.1002/kin.20867
- [14] Mehl M., Pitz, W.J., Westbrook, C.K., Curran, H.J., "Kinetic modeling of gasoline surrogate components and mixtures under engine conditions", *Proceedings of the Combustion Institute* 33:193-200 (2011).
- [15] Chen, J. Y., Blasco, J. A., Fueyo, N., Dopazo, C., "An economical strategy for storage of chemical kinetics: Fitting in situ adaptive tabulation with artificial neural networks", *Proceedings of the Combustion Institute*, Volume 28, Issue 1, 2000, Pages 115-121, ISSN 1540-7489, DOI: 10.1016/S0082-0784(00)80202-7
- [16] Pope, S. B., "Computationally efficient implementation of combustion chemistry using in situ adaptive tabulation", 1997, *Combustion Theory and Modelling*, DOI: 10.1080/713665229
- [17] Jach, A., Zbikowski, M., Malik, K., Żbikowski, M., Adamski, K., Cieślak, I., Teodorczyk, A., "Methane-air laminar burning velocity predictions with machine learning algorithms", 2017, 10.13140/RG.2.2.10390.86081
- [18] Géron, A., "Hands-on machine learning with Scikit-Learn and TensorFlow: concepts, tools, and techniques to build intelligent systems", Sebastopol, CA: O'Reilly Media. ISBN: 978-1491962299, 2017
- [19] Abadi, M., Barham, P., Chen, J., Chen, Z., Davis, A., Dean, J., et al. (2016) "Tensorflow: A system for large-scale machine learning", 12th USENIX Symposium on Operating Systems Design and Implementation (pp. 265–283)
- [20] Pedregosa, F., Varoquaux, Gaël, Gramfort, A., Michel, V., Thirion, B., Grisel, O., et al. (2011), "Scikit-learn: Machine learning in Python", *Journal of Machine Learning Research*, 12(Oct), 2825–2830
- [21] Freund, Y., Schapire, R., "A Decision-Theoretic Generalization of on-Line Learning and an Application to Boosting", 1995
- [22] Zhu, J., Zou, H., Rosset, S., Hastie, T., "Multi-class AdaBoost", 2009

[23] Hastie, T., Tibshirani, R., Friedman, J., “The elements of statistical learning: data mining, inference and prediction”, Springer, 2009

[24] Niemeyer, K.E., Sung, C.J., Raju, M.P., “Skeletal mechanism generation for surrogate fuels using directed relation graph with error propagation and sensitivity analysis”, Combust. Flame, 157(9):1760--1770, 2010. DOI: 10.1016/j.combustflame.2009.12.022